OPEN EUROPEAN JOURNAL ON VARIABLE STARS
July 2024 https://oejv.physics.muni.cz ISSN 1801-5964
DOI: 10.5817/OEJV2024-0252

One-year Photographic Light Curves of Supernova 2023ixf in Messier 101 from a Bortle Class 9 Sky

GONG, T. HAO[1]

1) Department of Chemistry and Biotechnology, Graduate School of Engineering, The University of Tokyo, 7-3-1 Hongo, Bunkyo-ku, Tokyo, Japan 113-8656 haggon.universe@gmail.com

Abstract: This work presents one-year photographic light curves of the Type II supernova (SN 2023ixf), discovered last year in Messier 101 galaxy (NGC 5457). The maximum apparent brightness was observed on day 5 after the estimated explosion with a magnitude of 10.7(0.16), based on red pixels that are responsive to wavelengths in the range of 570–1000 nm (full width at half maximum: 395 nm). Despite being collected in the center of a metropolitan area using a fully automated commercial robotic telescope, the light curves exhibit the characteristics of a Type II-P supernova, which are consistent with two recent reports from dedicated observatories. However, after a point-by-point comparison, two major differences were reported in this work. Namely, the light curves displayed a slightly more noticeable plateau and a significantly lower blue-band apparent brightness than the other two reports. These two differences are likely caused by more pronounced random errors and systematic errors, respectively, under a Bortle class 9 sky.

1 Introduction

Transient astronomical events, such as supernovae, occur randomly in deep space, typically at great distances within distant galaxies or in our Milky Way galaxy. It is common sense that to reduce the effects of light pollution, one needs to be far away from a city to observe such a once-in-a-lifetime event. However, with the assistance of modern imaging technology, which is designed to enhance light responsiveness in the near-infrared range, the effects of light pollution may be compensated. SN 2023ixf, a Type II supernova in Messier 101 (M101, NGC 5457), a nearby face-on spiral galaxy located at 6.9 ± 0.12 Mpc, approximately 22.5 million light-years, was first reported by Koichi Itagaki at 17:27:15 UT on May 19, 2023 (Itagaki, 2023). Subsequently, several publications provided even earlier color information (Yaron, 2023), offering valuable insights into this event. Upon noticing this report, I promptly allowed my commercial robotic observation station, situated on an open balcony in the central region of the Greater Tokyo Area with a population of 38 million, to point at the galaxy on the clear night of May 23, 2024. SN 2023ixf, invisible to the naked eye from here, was visible as a bright blue dot on a digital screen with just 10-second exposure. Encouraged by this, I set up the telescope at the same location every night for the next 300 days whenever the sky was clear. After collecting the data, I processed them by SIRIL, followed by analyzing the split color profiles of the SN alongside 12 nearby reference stars via IMAGEJ. Finally, I identified three reference stars to obtain the time-dependent light curves of the SN, complete with error bars. Despite the resemblance of the shape to two

DOI: 10.5817/OEJV2024-0252

reported data from dedicated observatories (Yang, 2024; Zimmerman, 2024), I recognized two differences in this work. These differences are likely caused by a random error, such as light/air pollution, under a Bortle class 9 sky (Bortle, 2001), as described in the final section.

2 Observation and Data Reduction

A total of thirty-one observations were conducted in Bunkyo-ku, Tokyo, Japan (35°42'46.1"N, 139°45'58.3"E) from May 23, 2023, to April 14, 2024, as listed in Table 1 with their respective time-spans. The visible photometric data of SN 2023ixf and its host galaxy was acquired by a robotic observation station Vespera-VE50 manufactured by VAONIS in France. This observation station affixed to a software-based de-rotation altitude-azimuth mount, is equipped with an apochromatic quadruplet lens featuring a focal length of 200 mm and a diameter of 50 mm. The imaging system utilizes a Sony IMX462 near-infrared enhanced one-shot color sensor (1920 × 1080) working at ambient temperature, integrated with the lens to provide a field of view of 1.6° × 0.9° with a sampling rate of 2.99 arcsec/pixel. According to the reported quantum efficiency curves of Sony IMX462, the red pixel responds to the light in the range of 570–1000 nm (full width at half maximum, FWHM: 395 nm), while the green and blue pixels respond to the light in the range of two distinct bands. Specifically, the green pixel is responsive to 475–610 nm (FWHM: 120 nm) and 700–1000 nm (FWHM: 230 nm), and the blue pixel is responsive to 400–520 nm (FWHM: 100 nm) and 750–1000 nm (FWHM: 190 nm). No additional filter was applied for all observations.

Table 1: Summary of observations on SN 2023ixf. All times are listed as starting times in UTC+9.

Session	Time-span [hours]	Session	Time-span [hours]	Session	Time-span [hours]
01:18 23 May, 2023	0.57	19:07 25 July, 2023	0.84	18:47 14 September, 2023	0.54
19:14 24 May, 2023	1.23	20:12 28 July, 2023	0.95	17:44 18 September, 2023	0.86
20:52 25 May, 2023	0.86	20:25 30 July, 2023	1.03	17:58 13 October, 2023	0.63
19:19 03 June, 2023	1.19	19:48 4 August, 2023	1.44	03:07 9 February, 2024	1.16
20:41 07 June, 2023	0.56	18:28 11 August, 2023	0.15	00:00 30 March, 2024	1.02
21:47 16 June, 2023	0.65	18:46 17 August, 2023	1.08	02:07 1 April, 2024	0.78
21:30 4 July, 2023	0.45	18:28 21 August, 2023	0.23	23:07 9 April, 2024	0.48
22:15 6 July, 2023	0.59	19:33 24 August, 2023	1.04	23:52 10 April, 2024	1.07
20:36 11 July, 2023	0.81	18:29 25 August, 2023	1.00	01:11 14 April, 2024	0.94
19:03 16 July, 2023	1.49	18:34 29 August, 2023	1.31		
19:42 23 July, 2023	1.23	18:13 5 September, 2023	0.97		

DOI: 10.5817/OEJV2024-0252

Three reference stars (TYC 3852-1069-1; TYC 3852-1108-1; TYC 3852-519-1) were used for calibration of the apparent magnitude of the SN. These stars are listed in Table 2 and highlighted within blue-colored circles in Figure 1.

Table 2: Characteristics of reference stars. Magnitudes are taken from SIMBAD (2024).

Star	ID	*RA* (h:m:s)	*DEC* (°:':")	*B* [mag]	*V* [mag]	*R* [mag]
Ref-1	TYC 3852-1069-1	14:04:21.68	+54:19:22.53	12.62(0.22)	12.44(0.21)	11.2(~)
Ref-2	TYC 3852-1108-1	14:03:49.86	+54:09:05.48	12.08(0.16)	11.48(0.12)	11.2(~)
Ref-3	TYC 3852-519-1	14:02:12.36	+54:31:33.76	12.32(0.19)	11.84(0.17)	11.2(~)

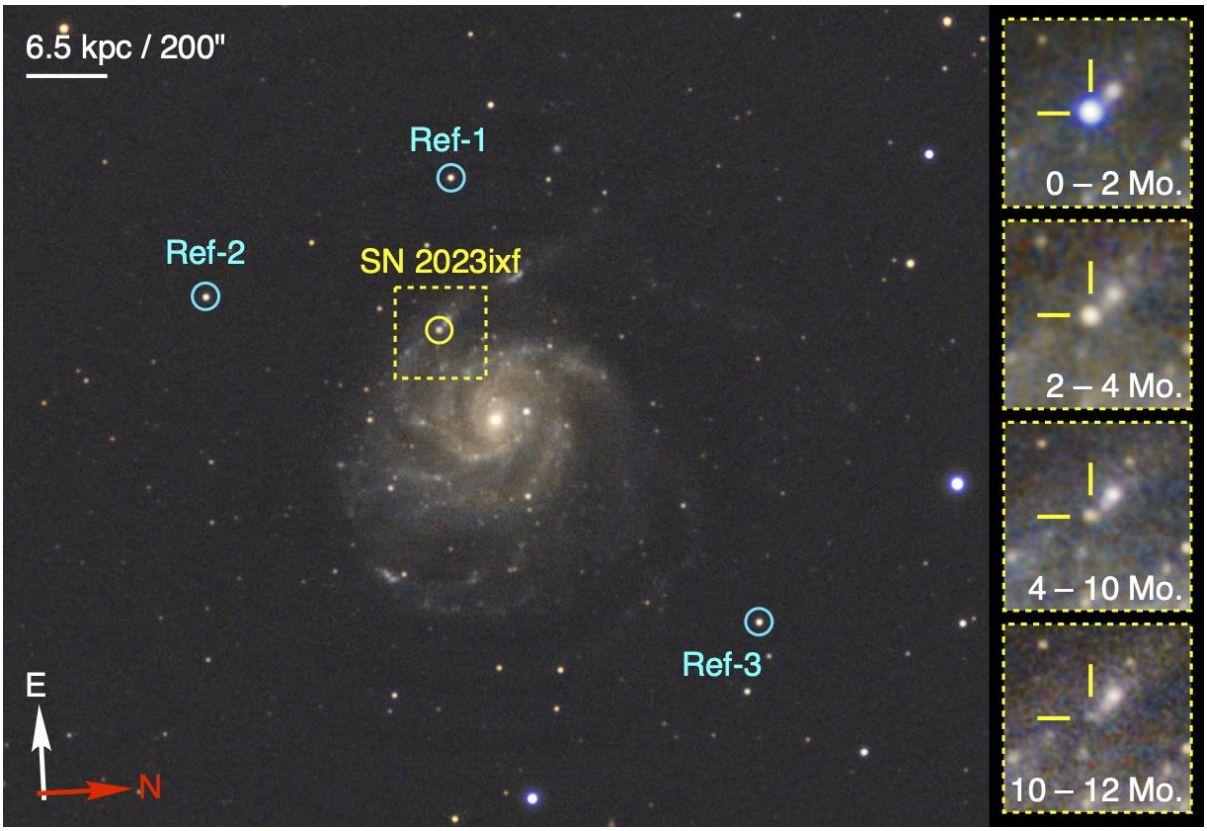

Figure 1: Photographic image of Messier 101 (M101, NGC 5457) processed by SIRIL using data from May 2023 to April 2024. Yellow-colored circle, Supernova 2023ixf. Blue-colored circles, Reference stars (TYC 3852-1069-1; TYC 3852-1108-1; TYC 3852-519-1). Scale bar, 200 arcseconds. Right, Photographic time-dependent change in the vicinity region of the supernova in the yellow-colored rectangular frame using different temporal data.

DOI: 10.5817/OEJV2024-0252

3 Data Analysis and Results

First, automatically aligned and stacked 16-bit TIFF files from each observation session were processed via Singularity (VAONIS) to eliminate defective pixels. Followed by the vignette correction process via a smooth background extraction in SIRIL (1.2.1), each 16-bit TIFF file underwent photometric color calibration and image plate-solving processes. Next, all images were 2× drizzled and aligned via automatic image registration to yield the calibrated 16-bit FITS files via SIRIL.

Consistent with the first report (Itagaki, 2023), the image of the host M101 galaxy, processed using one-year observational data, clearly depicts SN 2023ixf (Figure 1) on one of the spiral arms, with coordinates of Right Ascension 14h 03m 38.56s and Declination +54° 18' 42.13". Then, I noticed that the SN appears orange in Figure 1, but this SN is significantly bluer in the image processed using only the initial two-month data. Later, I found that the color shifted from blue to orange over the following two months (Figure 1, right), suggesting that the emitted light with a shorter wavelength decayed faster than that with a longer wavelength. To quantify this observation, time-dependent light curves in each color channel should be analyzed.

All calibrated color FITS files were split into three 16-bit grey profiles from red, green, and blue pixels, via IMAGEJ. Next, I extracted the maximum intensity values of SN 2023ixf and the other 12 reference stars in their respective cropped regions (20 × 20 pixels). To determine the absolute grey intensities of the stars in each color channel, I subtracted the mean grey intensity of the selected background region from each corresponding maximum grey intensity. By analyzing the time-dependent grey intensity changes of the SN, which were plotted in their normalized relative intensities by setting the maximum value as 100%, I selected three reference stars, out of the 12 stars, for further apparent brightness calculation. Subsequently, the apparent brightness in magnitude of SN was calculated by the following equation:

$$M_{SN} = M_{Ref} - 2.5 \times log_{10}\left(\frac{I_{SN}}{I_{Ref}}\right) \quad (1)$$

I_{SN} and I_{Ref} are the absolute grey intensities described above. M_{ref} is the magnitude of the reference star in the corresponding color bands, wherein the data from blue, green, and red pixels were respectively calculated by reported *B*, *V*, and *R* values in Table 2.

As shown in Figure 2, I constructed the light curves using 20:00 May 18, 2023 UT, as the starting time of the explosion, based on estimates contributed by amateur astronomers from around the globe (Yaron, 2023). For better visibility, three trend curves were added to Figure 2, and dashed curves were also included to represent the rising phase of the SN based on the reported observation data (Yaron, 2023; Zimmerman, 2024).

DOI: 10.5817/OEJV2024-0252

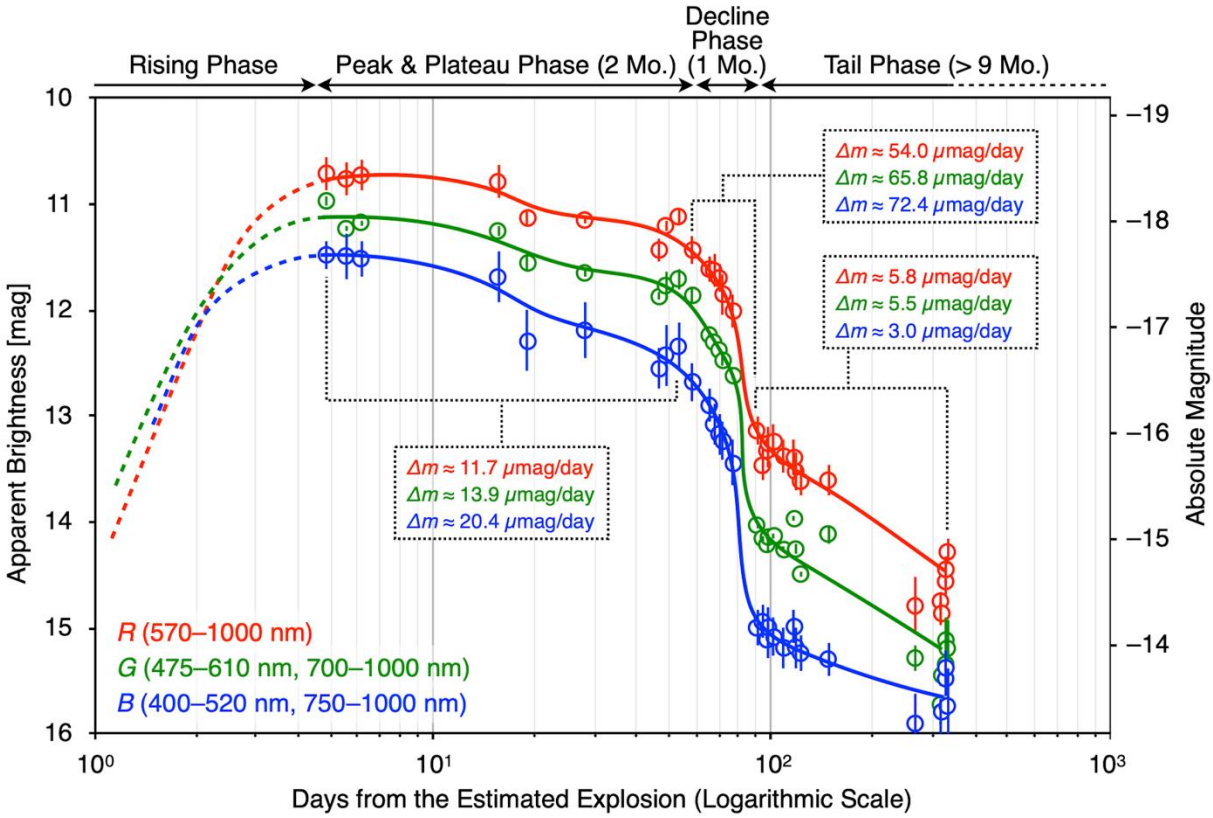

Figure 2: One-year photographic light curves (logarithmic scale) of Supernova 2023ixf. The vertical axes respectively represent the apparent brightness in magnitude (left) and the absolute magnitude derived from the distance to the host galaxy (right), while the horizontal axis represents days from the estimated explosion (Yaron, 2023). Broken lines correspond to reported light curves in the rising stage (Zimmerman, 2024), whereas solid lines are the trend lines of the data for clarity. The error bars originate from the calibration deviations using three different reference stars. All corresponsive decline rates for each transition phase are indicated within the dotted line frames. Red, green, and blue colors represent the data derived from the corresponding red, green, and blue pixels.

To my surprise, three light curves from the three-color pixels depicted the post-peak plateau region, a typical Type II-P supernova (Young & Branch, 1989; Filippenko, 1997), with a slow decline rate of ≈15.5 μmag/day fitted by a linear model. The maximum apparent brightness in magnitudes [Blue: 11.5(0.13), Green: 11.0(0.04), and Red: 10.7(0.16)] was observed on day 5 after the estimated explosion. Although the brightness values from blue pixels are significantly lower than those reported in most studies, the values from red pixels are more consistent with existing data (Birch, Devalapalli & Sowell, 2024; Yang, 2024; Zimmerman, 2024).

As shown in Figure 3, by point-by-point comparison with the light curves of the red bands in two recently published works (Yang, 2024; Zimmerman, 2024), two major differences were found. First, the light curves displayed a slightly more noticeable plateau. Namely, the light curve displayed a more pronounced drop at the early stage of the plateau (day 20) and a rise at the later stage of the plateau (day 50). Because the data points exhibited similar patterns across all bands, this indicated that random error, rather than systematic error, contributed to this

OPEN EUROPEAN JOURNAL ON VARIABLE STARS
https://oejv.physics.muni.cz
DOI: 10.5817/OEJV2024-0252
ISSN 1801-5964

deviation. Initially, I reckoned that this might be due to my evaluation method. Unfortunately, it was found that the pattern in all bands stayed the same by applying point spreading function (PSF) photometry. Then, I revisited the atmospheric conditions, such as temperature and humidity, during those observation periods, but found no clear relationship. Therefore, other atmospheric effects, different integration times, and even the complex circumstellar environment of the SN (Zimmerman, 2024) may be the cause of this phenomenon. The second difference was that the light curve in the red band showed about 0.3 magnitudes higher value than that in the two reports (Figure 3) because the red pixel used in this work had wider light band responsiveness, as described above.

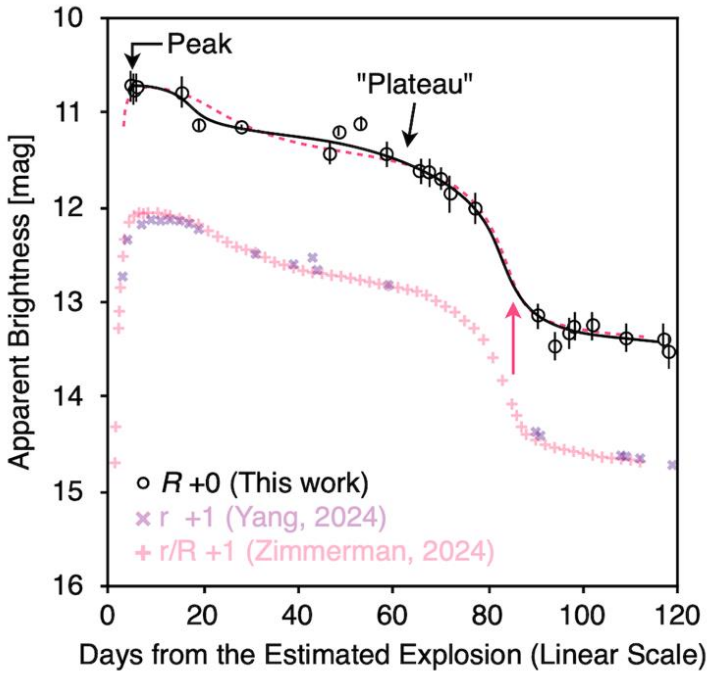

Figure 3: Comparison of light curves (linear scale) of Supernova 2023ixf in red bands between this work and two recently published works (Yang, 2024; Zimmerman, 2024). Offsets are added for clarity, as shown in the legend. The vertical axis represents the apparent brightness in magnitude, while the horizontal axis represents days from the estimated explosion (Yaron, 2023). The pink dashed curve from the work by Zimmerman et al. is aligned with the black line (this work) for comparison, displaying a slightly more noticeable post-peak plateau. The error bars originate from the calibration deviations using three different reference stars.

From the days 60 to 90 after the explosion, the SN gradually moved to the decline phase (Filippenko, 1997), which exhibited a faster decay behavior with an average linear decline rate of ≈62.1 μmag/day, suggesting characteristics of a Type II-P supernova. During this phase, the light curve from the blue pixels exhibits the greatest dimming, reaching an average magnitude of 15, compared to 13 and 14 for those from the red and green pixels, respectively, resulting in the observed blue-to-orange color change in Figure 1. After this phase, the light curves transitioned into a much slower decay phase with an average decline rate of ≈5.1 μmag/day, as

DOI: 10.5817/OEJV2024-0252

the average magnitude changed from 14 to 15 over the next 200 days until it was no longer detectable via my equipment. In this period, the light curves from red and green pixels (responsive to 500–1000 nm) displayed a slightly faster dimming behavior [Decline rates: ≈5.8 μmag/day (Red), ≈5.5 μmag/day (Green)] than that from the blue pixel (responsive to 400–500 nm and 750–1000 nm) (decline rate: ≈3.0 μmag/day), potentially due to the cooling of the high energy ejecta and the expanding radius of the remnant following the explosion (Woosley & Weaver, 1986).

4 Summary and Discussion

The one-year-dependent light change in SN 2023ixf presents the typical Type II-P supernova feature (Filippenko, 1997) with a peak and a single post-peak plateau phase, which lasts approximately two months, followed by a rapid decline phase over the subsequent month. Two major differences were found in this work, a slightly more noticeable plateau and a significantly lower blue-band apparent brightness value, where the first difference was likely caused by random errors from the observation. As for the second difference, the underestimation of the magnitude values from blue pixels is likely due to the absorption of high-energy blue light by the molecules in the atmosphere, such as nitrogen dioxide, a known UV-to-blue band (300–490 nm) absorber (Merienne, Jenouvrier & Coquart, 1995) and one of the most important molecules causing urban air pollution. Accordingly, this difference could be caused by a systematic error from the Bortle class 9 sky, which could be reduced through a more precise photometry calibration method. To compensate for the effects of light pollution, a one-shot color sensor is usually designed with pixels capable of responding to a wide range of wavelengths or even double broadbands. However, what one can conclude from such a design is limited. A one-shot color sensor with three traditional RGB pixels plus one near-infrared enhanced monochrome pixel would be more beneficial, since this would enable the acquisition of blue (B), visible or green (V/G), red (R), and near-infrared (I) bands, aligning with the standard photometric system (Bessell 2005) for more detailed analysis.

It should be noted that the zenith sky brightness of the place (9.65 mcd/m^2) for this work is 54 times brighter than that of the location (0.18 mcd/m^2) situated at an altitude of 2300 m above sea level where Liverpool telescope, responsible for obtaining the light curves of the SN for initial ~100 days (Zimmerman, 2024), is located. Interestingly, a detailed comparison between this work collected in a metropolitan center and two reported light curves from dedicated telescopes at a remote mountaintop, despite a small deviation caused by more random errors, reveals basic consistency in shape. This highlights the great potential contributions to transient astronomical events by any observers regardless of location.

Acknowledgments: I want to thank the Molecular & Life Innovation Building at the University of Tokyo for providing an open balcony for observation.

DOI: 10.5817/OEJV2024-0252

References

Birch, M., Devalapalli, P., Gautam, A. & Sowell, J. R., 2024, OEJV, 247.
https://ui.adsabs.harvard.edu/search/2024OEJV..247….1B/

Bessell, M. S. 2005, ARA&A, 43, 293
https://ui.adsabs.harvard.edu/abs/2005ARA%26A..43..293B/

Bortle, J. E., 2001, Sky and Telescope.
https://ui.adsabs.harvard.edu/abs/2001S%26T…101b.126B/

Filippenko, A. V., 1997, ARA&A, 35, 309
https://ui.adsabs.harvard.edu/abs/1997ARA%26A..35..309F/

Itagaki, K. 2023, Transient Name Server Discovery Report, 2023-1158, 1
https://ui.adsabs.harvard.edu/search/q=2023TNSTR1158....1I/

Merienne, M. F., Jenouvrier, A. & Coquart, B., 1995, Journal of Atmospheric Chemistry, 20, 281 https://doi.org/10.1007/BF00694498

SIMBAD, 2024 https://simbad.cds.unistra.fr/

Sony IMX462 quantum efficient curves
https://www.argocorp.com/cam/ImagingSource/sensor/Sony_IMX462.html

Woosley, S. E. and Weaver, T. A., 1986, ARA&A, 24, 205
https://doi.org/10.1146/annurev.aa.24.090186.001225

Yang, Yuan-Pei., Liu, Xiangkun., Pan, Yu., et al. 2024, arXiv:2405.08327
https://ui.adsabs.harvard.edu/abs/2024arXiv240508327Y/

Yaron, O., Bruch, R., Chen, P., et al. 2023, Transient Name Server AstroNote, 133, 1
https://ui.adsabs.harvard.edu/search/q=2023TNSAN.133….1Y

Young, T. R., & Branch, D. 1989, ApJL, 342, L79
https://ui.adsabs.harvard.edu/abs/1989ApJ…342L..79Y/

Zimmerman, E. A., Irani, I., Chen, P., et al. 2024, Nature, 627, 759
https://ui.adsabs.harvard.edu/abs/2024Natur.627..759Z/